Influence of Solvent and Crystalline Supramolecular Structure on the Formation of Etching Patterns on Acetaminophen Single Crystals: A Study with Atomic Force Microscopy and Computer Simulation

Tonglei Li, Kenneth R. Morris, and Kinam Park*

Department of Industrial and Physical Pharmacy, School of Pharmacy, Purdue University, West Lafayette, Indiana 47907-1336

Received: August 23, 1999; In Final Form: December 8, 1999

Understanding the evolution of surface morphology or surface texture of molecular crystals by dissolution/etching may be useful in determining the dissolution mechanisms at the molecular level. In this study, partial dissolution tests were conducted on the (010) face of acetaminophen single crystals with selected solvents: water, dichloroethane, pyridine, acetone, ethyl acetate, and acetic anhydride. Surface textures and etching patterns were examined with an atomic force microscope (AFM). It was found that etching patterns were regular and their shape depended on the solvent used for the etching. The etching patterns observed were parallelogram (by water and acetic anhydride), slit (by dichloroethane), hexagonal (by pyridine), square (by acetone), or rectangular (by ethyl acetate). It seems that all etching patterns are related to the underlying crystal structure. The crystal structure was used in simulation of the dissolution process by a computer model. Two essential events were considered during the simulation, detachment of crystal molecules, and surface diffusion of the desorbed molecules. Simulation results indicated that surface diffusion played the key role in forming etching patterns. The surface diffusion was thought to be guided or confined by the underlying crystal structure, especially the supramolecular interaction network. The discrepancy in the etching patterns between the simulation results and some of the experimental observations was explained by adsorption of solvent molecules on the crystal surface. It was likely that the adsorption of solvent molecules changed or interrupted the original interaction network within the crystal structure, leading to the mutation of the etching pattern. Our study indicated that the etching pattern at the crystal surface was influenced not only by the solvent−solid interaction but also by the crystal structure and the mutual recognition between solvent molecules and crystal molecules.

Introduction

Changes in surface morphology of crystals during crystallization or dissolution processes have been extensively studied.[1,2] Understanding the formation of surface morphology is important since it sheds light on the interaction between the crystals and their environment and on the mechanism of crystal growth and/or dissolution. We were interested in understanding the crystal dissolution process and, in particular, the mechanisms of the formation of surface morphology, or etching pattern, during dissolution.

Dissolution is a physicochemical process by which a solid substance goes into at least a binary solution. Generally, dissolution can be regarded as a specific type of heterogeneous reaction between the solid and the solvent.[3] Solvent molecules first adsorb onto the crystal surface. Then, interaction/reaction occurs between the crystal and adsorbed solvent molecules. Finally, the reaction products (i.e., solubilized molecules) detach and diffuse away from the surface. This dissolution scheme led to treatment of the dissolution process as a transport-limited process,[4] a surface-controlled process,[5] or a mixed transport-surface process.[6] These models, however, were not designed to treat the mechanism of dissolution at the molecular level.

Formation of a surface morphology and an etching pattern during dissolution is a result of the interaction between solvent molecules and solid molecules at the interface. The terrace−ledge−kink (TLK) model has been used to describe crystal growth and dissolution.[7] In this model, five different sites (adatom, ledge, kink, step, and terrace) can exist on the crystal surface defined by the number of nearest neighbor molecules. Three elementary processes, adsorption, detachment, and surface diffusion are thought to be common to crystallization and dissolution (Figure 1). Thus, dissolution can be considered as a process where kinks move along steps until the receding steps reach the edge.[8] The screw dislocation, two-dimensional (2D) nucleation process (i.e., formation of a vacancy on the crystal surface), and defects are regarded as sources of new steps. The degree of solute saturation and the energy changes caused by the elementary processes determine the surface topography and morphology.[9] The adsorption of solvent molecules is controlled by the chemical potential difference between the solid and liquid phases. The energy change associated with detachment of crystal molecules is related to the interaction between solid and liquid. Surface diffusion is very common and easy to activate, and it is believed to be the main factor causing surface reconstruction.[10−12]

It is possible to establish continuum equations for the evolution of surface topography as a function of the dissolution time. The equations can be solved analytically. The Kardar−Parisi−Zhang (KPZ) equation is used to describe surface changes by random deposition with surface relaxation.[13] Surface

* Corresponding author. Phone: (765) 494-7759. Fax: (765) 496-1903. E-mail: esp@omni.cc.purdue.edu.

10.1021/jp992967z CCC: $19.00
Published on Web 02/10/2000

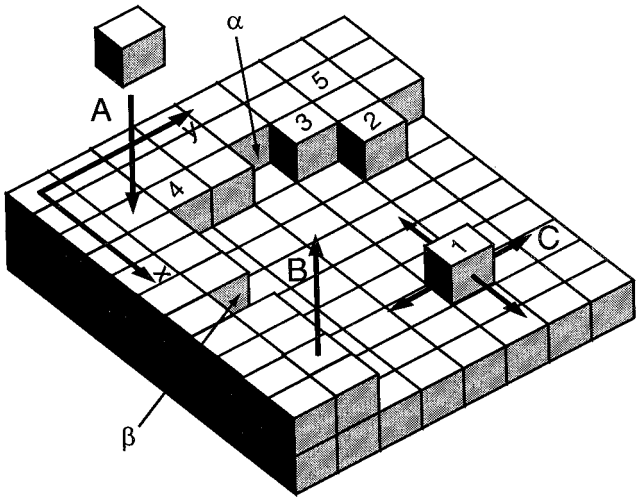

Figure 1. Terrace−ledge−kink model for crystal growth and dissolution. Three essential molecular events are believed to control the mechanisms: adsorption (A), detachment or desorption (B), and surface diffusion (C). According to the number of nearest neighbors, surface molecules can be categorized as adatom (#1), ledge (#2), kink (#3), step (#4), and terrace (#5). Two empty sites are marked by α and β which #1 may diffuse and occupy.

diffusion can be included into the KPZ equation.[14] Using continuum equations to solve crystal growth and dissolution, however, may be impossible if the elementary processes are anisotropic.[15] In fact, anisotropic diffusion behavior is common on crystal surfaces.[10]

Computer simulation may have a potential to explain some of the experimental observation on the dissolution of molecular crystals and help deduce the underlying mechanisms. This is especially important given the fact that the molecular interactions in molecular crystals are generally anisotropic. The advantage of computer simulation over numerical and analytical methods is that once the basic mechanisms of molecular events are found or assumed, the complicated, large-scale structural features can be generated. Simulation of crystal dissolution was reported as early as the 1970s.[16,17] Movements of surface molecules such as detachment and simple schemes of surface diffusion were considered. Recent studies take into account more complicated events such as diffusion bias.[18] However, there has been no significant computer simulation work reported for more complicated systems such as molecular crystals.

Recent advances in scanning probe microscopy (SPM) made it possible to verify the simulation results experimentally and check the hypothesized mechanisms of dissolution. Atomic force microscope (AFM) and other SPM techniques are ideally suited to study the dissolution process. Dissolution is a heterogeneous reaction occurring on the surface, and AFM is able to image three-dimensional (3D) surface profiles at the nanoscopic scale.[19,20] It is not surprising that AFM has been widely used to observe various surface phenomena including dissolution.[18,21−23] AFM experiments of the dissolution process help design better models for computer simulations. In turn, the results of computer simulation can help interpret the experimental data. These iterations will help decipher the dissolution mechanisms. Given the increasing computational power, the simulation results will become closer and closer to the experimentally observed data.

We studied the evolution of surface morphology of acetaminophen single crystals after partial dissolution with selected solvents on the cleaved (010) face. AFM was used to examine the microscopic etched patterns, and a computer model was employed to explore possible dissolution mechanisms that

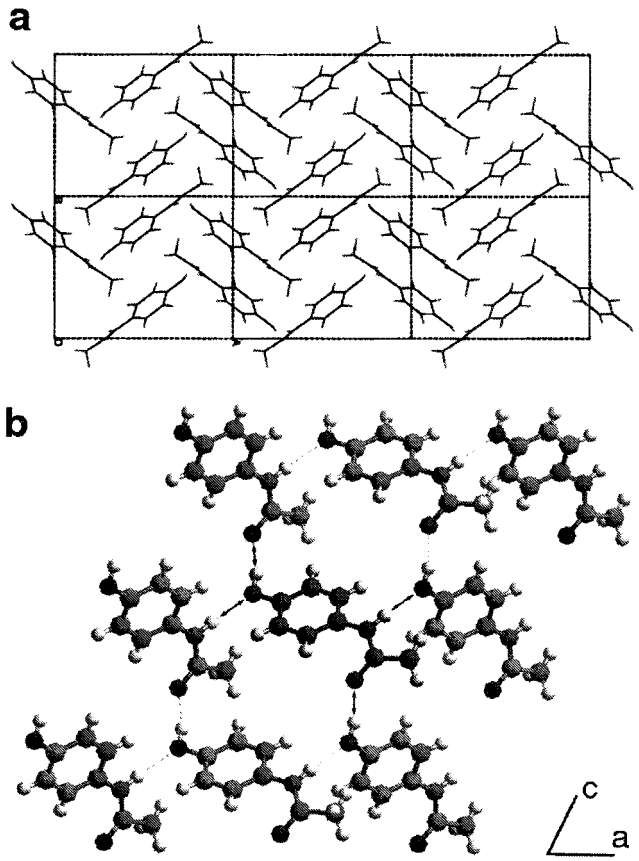

Figure 2. Crystal structure of acetaminophen. The layering structure can be seen from the (110) face (a) and no hydrogen-bonding interaction exists between layers. On the (010) face (b), there is a 2D hydrogen-bonding interaction network where a molecule is bound through four hydrogen bonds. One hydrogen-bonding direction is along the *a* axis. Another one is between the *a* and *c* axes. No hydrogen bonding along the *c* axis.

caused the specific surface morphology or etched pattern. Acetaminophen is a molecular crystal[24] with a large number of weak, noncovalent intermolecular interactions (especially hydrogen bonding) that maintain the supramolecular motifs in crystal structures. The acetaminophen crystal can be described as stacked 2D layers through van der Waals interactions with stronger intermolecular interactions (i.e., hydrogen bonding) within the layer (Figure 2). This layering structure feature is common for molecular crystals.[25,26] Because of the large number of anisotropic intermolecular interactions, the surface morphology created by etching of acetaminophen single crystals may reveal information about the dissolution mechanisms.

Experimental Methods

Crystal Growth. Singles crystals tested in the study were grown in the laboratory. Acetaminophen raw materials (USP/BP, Hoechst Celanese, Bishop, TX) were used for crystal growth. On the basis of the solubility of acetaminophen (19−20 mg/mL at 37 °C and 11.6−14.5 mg/mL at 25 °C),[27] 9 g of raw materials was dissolved in 500 mL water at 37 °C in a 4000 mL crystallizer (Lab Glass, Vineland, NJ). This represents a supersaturation ratio of ∼124−155% at 25 °C. The solution was stirred for 5 h and then left undisturbed to cool to 25 °C. Starting from 35 °C, the temperature of the water bath was cooled 1 °C at each step and was held at that temperature for at least 4 h. Approximately 150 mL of solvent was evaporated by the end of the experiment. Low suction filtration was used

to harvest the crystals. In all, 3 g of single crystals were obtained and air-dried.

Powder X-ray Diffraction (PXRD) Measurement. Well formed single crystals were harvested after the crystallization. Acetaminophen crystals had to be cleaved to expose the (010) face. In fact, the (010) face is the only reported slip plane.[28] To verify the indices of the face, about half the cleaved faces were identified by a powder X-ray diffractometer (PXRD) (XRD-6000, Shimadzu, Japan). The area of the (010) face was normally around 1×1 mm^2. Attention was paid to picking good samples for the PXRD and subsequent dissolution tests. After cleaving, the (010) face of single crystals was checked under the microscope for flatness. As large as possible a single layer of the (010) face was needed. The cleaved single crystal was mounted on the PXRD sample holder with double-sided scotch tape. The scan range covered from 5° to 45° with step size of 0.02°. The voltage and current of PXRD were set at 40.0 kV and 40.0 mA, respectively. If the (010) face was not parallel to the plane of the sample cell, the θ oscillation mode was used to bring the face into diffracting position.

Axes Identification. Because the dissolution tests were conducted on the (010) face of acetaminophen single crystals, it was necessary to identify the *a* and *c* axes ([100] and [001]) to correlate etch pits with the underlying crystal structure. This was done by analyzing the morphology of the (010) face on which three different angles exist: 117.8° between (−201) and (001), 126.3° between (200) and (20−1), and 115.9° between (001) and (200). Since these faces were perpendicular to the (010) face, the measured angles were the angles of the hexagonal face. The *a* and *c* axes was identified by measuring each angle on (010) face. During the AFM measurement, the image of the (010) face was obtained with an optical microscope and relayed to a TV monitor. The hexagon of the (010) face was printed on a transparency and put on the TV screen to identify angles.

Partial Dissolution. Several solvents were chosen for dissolution tests on cleaved (010) faces of acetaminophen. The solvents used included deionized distilled water, acetone (EM Science, Gibbstown, NJ), acetic anhydride (Mallinckrodt Baker, Pairs, KY), pyridine (Fisher Scientific, Fair Lawn, NJ), ethyl acetate (Mallinckrodt Baker, Pairs, KY), 1,2 dichloroethane (Mallinckrodt Baker, Pairs, KY), and carbon tetrachloride (Sigma Chemical, St. Louis, MO). The dissolution time normally ranged from a few seconds to a few minutes depending on the solubility of acetaminophen in the solvent. For each experiment, a new, cleaved single crystal was mounted on the AFM sample holder, a metal disk, with either double-sided scotch tape or a tiny drop of Epoxy (ITW Devcon, Danvers, MA). The cleaved (010) face was leveled horizontally on the metal holder. The sample was attached tightly, so as not to loosen during the dissolution test. For water, the dissolution tests were carried out in a beaker submerged in a temperature-controlled water bath. For other solvents, tests were done at 20 °C. At a preset time point, the disk was removed from the solution and most of the solvent was removed using a filter paper. The residual solvent remaining on the crystal surface was removed with compressed air. The sample was then air dried overnight before AFM observation. Experimental conditions used for dissolution are listed in Table 1.

Solubility Measurement. The solubility of acetaminophen in dichloroethane, water, ethyl acetate, acetic anhydride, acetone, and pyridine was measured at 20 °C. An excess of acetaminophen single crystals was added to 100 mL of solvent in a beaker, which was then sealed. After the solution was stirred for 30 min, the beaker was submerged in a temperature-controlled water bath for 4 h at 25 °C. The solution was filtered into a graduated cylinder to measure the volume of the clear solution. The solution was then transferred into a tared crystallization dish. The dish was air-dried at 20 °C until constant weight was reached, up to 6 days. This method of measuring the solubility was adequate enough to provide relative solubility information. The measured solubility values are listed in Table 2.

TABLE 1: Solvents and Experimental Conditions of Dissolution Tests

solvent	duration (s)	temperature (°C)
H_2O	15, 30, 300, 600	30
H_2O	30, 60, 300, 600	40
$ClCH_2CH_2Cl$	15, 30, 60	20
C_5NH_5/CCl_4 (1:5 v/v)	5, 15, 30	20
CH_3COCH_3	15	20
CH_3COCH_3/CCl_4 (1:1 v/v)	5, 10, 15	20
$CH_3COOC_2H_5/CCl_4$ (1:1 v/v)	5, 15, 30	20
$(CH_3CO)_2O/ CCl_4$ (1:1 v/v)	5, 10, 20, 30	20

TABLE 2: Solubility of Acetaminophen in the Selected Solvents, Molecular Volumes of These Solvents, and the Shape of Etched Pits Formed in Each Solvent

solvent	solubility (mg/mL)	volume[a] (Å^3)	shape of etched pits
dichloroethane	0.2	76	slit
ethyl acetate	8	94	rectangle
acetic anhydride	9	96	parallelogram
water	14	20	parallelogram
acetone	84	66	square
pyridine	472	82	hexagon

[a] Calculated from the volume confined by Connolly Surface with Cerius^2. The probe radius was set as 1.0 Å. The molecular volume of acetaminophen is 135 Å^3.

AFM Measurement. The surfaces of the cleaved, etched (010) faces of acetaminophen single crystals were observed with an AFM (NanoScope Multi-Mode AFM, Digital Instruments, Inc., Santa Barbara, CA). AFM scans were carried out mostly in contact mode in air at 20 °C. The tips being used were standard silicon nitride probes from Digital Instruments, Inc. The resolution of all measurements was 512×512 points with equal steps along the *x* and *y* directions. Two scanners were used: E scanner with 10 μm lateral and 2.5 μm vertical range; J scanner with 125 μm lateral and 5 μm vertical range. Measurements were saved and images were exported for further analysis. For the AFM images shown in the following sections, unless otherwise stated, they were created by AFM system software in the deflection mode, which is the derivative along the scan directions of the surface profile.

Computer Simulation

Simulation Model. The crystal structure of acetaminophen available in the literature[24] was used to build a 3D-lattice model simulating the (010) face. In the model, each lattice point (or equivalently, a lattice box) represented an acetaminophen molecule, or one asymmetric unit in this case (Figure 3). The surface model was oriented to expose the (010) face on the top. If a molecule was dissolved, the representing lattice box was removed from the surface model. This model ignored the conformation and the orientation of each molecule. As indicated later, however, the energy calculation was carried out with the original crystal structure. In addition, the 2.35 Å horizontal shift between the two layers within one crystal lattice layer along the *b* axis (i.e., the horizontal shift between the centers of mass of corresponding molecules) was ignored. All layers were treated as if stacked evenly.

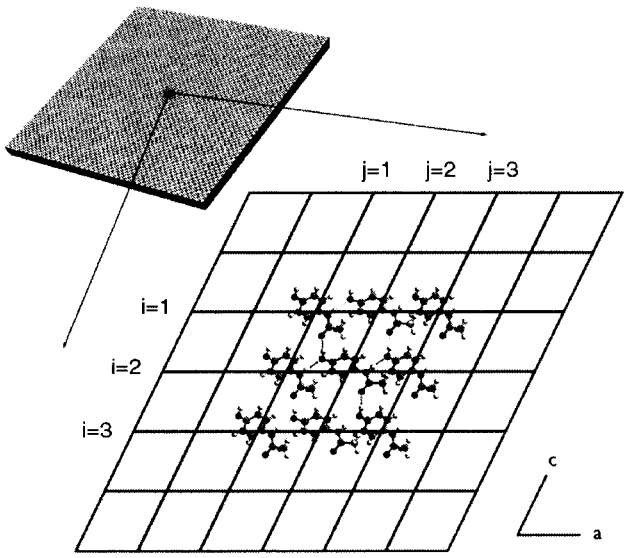

Figure 3. Simulation model of the (010) face of acetaminophen single crystal. The indexing is used to calculate the force matrix of the central molecule (Table 3).

Although the model was simplified, the interactions among all molecules were calculated based on the original crystal structure with Cerius[2] 3.5 (Molecular Simulation, Inc., San Diego, CA). The single-crystal structure of acetaminophen was retrieved from Cambridge Structural Database (HXACAN01) with the following cell constants: $P2_1/n$; $a = 12.93$ Å; $b = 9.40$ Å; $c = 7.10$ Å; $\beta = 115.9°$. The force field used was Dreiding 2.21. Partial atomic charges were computed with charge equilibrium method, Gasteiger-Quanta 1.0, in Cerius[2]. The interactions calculated included van der Waals interaction, Coulomb force (with the Ewald summation), and hydrogen bonding. Only adjacent molecules were considered when calculating interaction energies of a molecule. To calculate the intermolecular interactions between two molecules, the total energies of one acetaminophen molecule were calculated first. The total energy included van der Waals, Coulomb, hydrogen bonding, and all bonded energies. These were intramolecular interactions. Then, the two molecules were copied from the acetaminophen crystal structure and pasted into a new empty workspace to keep their distance and relative orientation as in the crystal. Periodic boundary conditions were discarded, so the two molecules were treated as in a vacuum. Total energies of the new system were calculated. The total intermolecular energies were determined by subtracting twice the intramolecular energies from the new values. For a given molecule, the intramolecular interactions with all its neighbors in the simulation model made up a $3 \times 3 \times 3$ matrix called a "force matrix" (Table 3). During a simulation, the interaction of a molecule with its neighbors was evaluated with a $3 \times 3 \times 3$ matrix. In this matrix, each element was either 0 or 1 to indicate an empty site or a molecule being at that neighbor position. This matrix was then applied to screen the force matrix to obtain the total value of the molecule. The force matrix was identical to the one generated from periodic bond chain (PBC) theory for connected nets.[29]

The force matrix in Table 3 shows that the total interaction value of a molecule with its neighbor molecules within the same layer (the middle layer in the force matrix) is −15.1228 kcal/mol. The total value with neighboring molecules in either the top or bottom layer is −11.3468 kcal/mol. Table 3 also shows that the interaction along the *a* axis is the strongest. This direction overlaps one of two hydrogen-bonding networks. The total interaction along another hydrogen bonding route is smaller than that along the *c* axis where no hydrogen bonding exists. This is due to a huge repulsive van der Waals force canceling out the largest hydrogen-bonding interaction. The distance between a hydrogen atom of a $-CH_3$ group of one molecule and a hydrogen atom of an −OH group of another molecule is close (about 2.4 Å). The interaction values between a molecule and its closest neighbors also show the anisotropy of the interaction network in the acetaminophen single crystal.

Random Walk. The Monte Carlo simulation method was utilized to study the formation of the etching pattern. The scheme to change system states, i.e., random walk, was set up based on the two molecular events considered in the simulation: desorption of crystal molecules and surface diffusion of desorbed molecules. The kernel of the algorithm was a loop of detachment and surface diffusion. After each detachment event, a number of diffusions were carried out. The framework of simulation programs consisted of these steps: (1) read parameters from the configuration file; (2) initialize the surface model; (3) apply Metropolis rule to remove a surface molecule (Loop); (4) allow a number of surface molecules to migrate to more stable sites; (5) repeat the loop.

Periodic boundary conditions were implemented in simulation so that surface models were considered infinite along horizontal directions. When a surface molecule was randomly chosen to be detached, the energy change of the molecule was computed. The Metropolis rule[30] was then applied to decide whether this site was removed from the surface. The energy change of a detached molecule was calculated from $\Delta E = \phi_{sl} - \phi_{ss} - \phi_{ll}$ where ϕ_{ss}, ϕ_{sl}, and ϕ_{ll} were solid−solid, solid−liquid, and liquid−liquid interactions, respectively. Because we did not consider the adsorption of solvent molecules to the empty site after a solid molecule dissolved, the interaction between the adsorbed solvent molecule(s) and surface solid molecules was ignored in this equation. The solid−solid interaction was specified by the force matrix (about −37.8 kcal/mol for a

TABLE 3: Interaction Values of a Molecule with Its Nearest Neighbors[a]

	$j = 1$ (kcal/mol)	$j = 2$ (kcal/mol)	$j = 3$ (kcal/mol)
$i = 1$	$-2.2521 - 0.3744 + 0 = -2.6264$	$-1.2036 - 0.2831 + 0 = -1.4867$	$-0.0086 + 0.0178 + 0 = 0.0092$
$i = 2$	$-0.7462 - 0.8263 + 0 = -1.5725$	$-4.9479 + 0.0659 + 0 = -4.8820$	$-0.9264 + 0.0264 + 0 = -0.9000$
$i = 3$	$0.0001 - 0.4010 + 0 = -0.4009$	$-0.0246 + 0.1391 + 0 = 0.1145$	$-0.0690 + 0.4671 + 0 = 0.3981$
$i = 1$	**$4.0114 - 1.3569 - 3.2582 = -0.6037$**	**$-0.8390 - 0.3188 + 0 = -1.1578$**	**$-0.0019 + 0.0909 + 0 = 0.089$**
$i = 2$	**$-1.3019 - 1.6255 - 2.9615 = -5.8889$**	**n/a**	**$-1.3019 - 1.6255 - 2.9615 = -5.8889$**
$i = 3$	**$-0.0019 + 0.0909 + 0 = 0.089$**	**$-0.8390 - 0.3188 + 0 = -1.1578$**	**$4.0114 - 1.3569 - 3.2582 = -0.6037$**
$i = 1$	$-0.0690 + 0.4671 + 0 = 0.3981$	$-0.0246 + 0.1391 + 0 = 0.1145$	$0.0001 - 0.4010 + 0 = -0.4009$
$i = 2$	$-0.9264 + 0.0264 + 0 = -0.9000$	$-4.9479 + 0.0659 + 0 = -4.8820$	$-0.7462 - 0.8263 + 0 = -1.5725$
$i = 3$	$-0.0086 + 0.0178 + 0 = 0.0092$	$-1.2036 - 0.2831 + 0 = -1.4867$	$-2.2521 - 0.3744 + 0 = -2.6264$

[a] Calculated with Cerius[2] 3.5. The interaction values in the three bold rows are for the middle layer. The upper and lower three rows are for the top and bottom layers of the force matrix, respectively. The indexing is shown in Figure 3. Each item includes van der Waals, Coulombic, and hydrogen bonding energies.

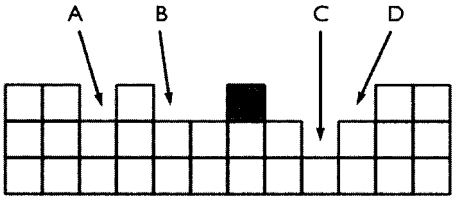

Figure 4. 2D demonstration of three defined surface diffusion modes. Each molecule is depicted as a square, and the gray one is a diffusing molecule. Empty sites (A, B, C, and D) are possible targets.

molecule inside the crystal). The other two terms were specified arbitrarily according to conditions to be simulated. In simulations reported here, the liquid−liquid interaction was assigned −10 kcal/mol, and the solid−liquid interaction was varied from −30 to −50 kcal/mol (correspondingly, the success ratio of detachment ranged from 1% to 100%) to test how the solvent quality affected the etching patterns.

For surface diffusion, three types of random walks were defined. After a surface site was dissolved, a number of surface molecules in an area around the dissolved site were subject to surface diffusion. The number of surface molecules and the size of the area for choosing diffusing molecules defined the frequency of the diffusion event over the detachment event. For each diffusing molecule, all the unoccupied sites around this molecule within a specified distance were examined. The distance defined the maximum diffusion length. An energetically favored site was identified for the diffusing molecule to occupy. If more than one site could reduce the energy, the most stable one was picked. If more than one could reduce the energy to the same extent, then a site among them was chosen randomly. This was the "strong diffusion" mode, which did not consider whether there was a diffusion path between the diffusing molecule and the energetically favored unoccupied surface site. It was assumed that the diffusing molecule somehow was able to find its way to the low-energy position. There were two options to control the interlayer diffusion or jumping. Normally, empty sites that were not higher than the diffusing molecule were considered. There was an option in the configuration file, however, to allow molecules to jump up to a higher layer ("jumping up") in the simulation. There was another option to allow "jumping down" to a lower layer. If these options were not allowed in a simulation, surface diffusion was allowed only within the same layer where the diffusing molecule was.

The second surface diffusion mode, called the "medium diffusion" mode, considered the diffusion path. After a stable site was identified for the diffusing molecule to move, the breadth-first search algorithm was used to find the shortest path between the two sites.[31] If there was no such path or an available path was longer than the maximum distance allowed, the empty site was rejected and the next candidate was considered. A diffusion path was defined as a route that led the diffusing molecule to the empty site without "climbing up" other surface molecules. The route might go down if the "jumping down" option was enabled. In the third mode, called the "weak diffusion" mode, a molecule around the just-dissolved site was chosen to carry out the surface diffusion. The diffusing molecule, however, picked a more or equally stable empty site to migrate only to its nearest neighbors. It was called "weak" because in the next step the molecule could migrate back to the original site. This move was repeated, and the number of repetitions was defined by the maximum diffusion length. Compared with the first two diffusion modes, this scheme, similar to a local thermal equilibration, achieved shorter diffusion paths. Figure 4 schematically summarizes these three diffusion modes. In the strong diffusion mode, the diffusing molecule will pick empty site A to occupy. If the "jumping down" option is enabled, sites A and C will be randomly selected. In the medium diffusion mode, the molecule will go to site B. Site D is rejected since there is no diffusion path. If the "jumping down" option is enabled, the molecule will go to more stable site C than site B. In the weak diffusion mode, the molecule moves to either the right or the left empty site.

As stated earlier, three select parameters were used to control the surface diffusion in simulation. It was assumed that there were more surface diffusion events than detachment events. Therefore, the programs executed a number of surface diffusions after each successful detachment. The frequency of the surface diffusion was specified by two parameters: diffusion area (i.e., the size of area around the dissolved site) and diffusion number (i.e., the number of surface molecules in this area subject to surface diffusion). The third parameter, called diffusion length, was used to specify the maximum diffusion length. In the strong and medium diffusion modes, the diffusion length defined the size of the area around the diffusing molecule where the simulation program searched for a proper empty site to migrate to. In the weak diffusion mode, however, the diffusion length was the number of repetition for the local vibrating move. In addition, as mentioned above, there were two relevant options: jumping up and jumping down. All these parameters were assigned proper values in the configuration file before starting a simulation.

Several programs were developed allowing simulation and visualization of simulated models. The coding was done in ANSI C on an IBM RISC/6000 workstation. Because of the limited computer power available, the model size and the number of simulations were restricted. The results reported here were collected from simulations of the model size of $6 \times 80 \times 80$ (layer × row × column).

Results

AFM Observation. Four AFM images of etched (010) faces of acetaminophen single crystals after exposure to water are shown in Figure 5. The etching pattern appears to be regular. There are two kinds of ledges formed on the surface along the *a* axis and *c* axis. These two kinds of ledges interconnect and the etch pits form parallelograms. The etch pits are more clearly shown in parts c and d of Figure 5. The parallelogram has two sides parallel to the *a* axis and the other two parallel to the *c* axis. It is common to observe that a big pit contained a few small ones (Figure 5d). It is noted that the axes in parts a and b of Figure 5 are enantiomers (as are the axes in parts c and d of Figure 5). This is due to the cleavage. After cleavage of a single crystal, the (010) faces of two halves of the single crystal are enantiomorphic (i.e., mirror images). Although the four surfaces in Figure 5 were not from the same single crystal, they happened to be mirror faces. Moreover, the measurements indicate that the duration and temperature of the dissolution process used in this study have little effect on the shape of the etching pattern. These two factors do, of course, affect the dissolution kinetics and amount of material dissolved.

Two images of the same etched (010) face of acetaminophen after being partially dissolved in dichloroethane show etch pits elongate along the *c* axis (Figure 6). Each one resembles a long, narrow cut on the crystal surface. The slits are perfectly aligned with the *c* axis. Interestingly, it seems that the *a* axis may not control any surface feature. At the small scale, the texture created by dissolution seems random (Figure 6b). Figure 7 shows two AFM images of the same cleaved (010) face of an acetami-

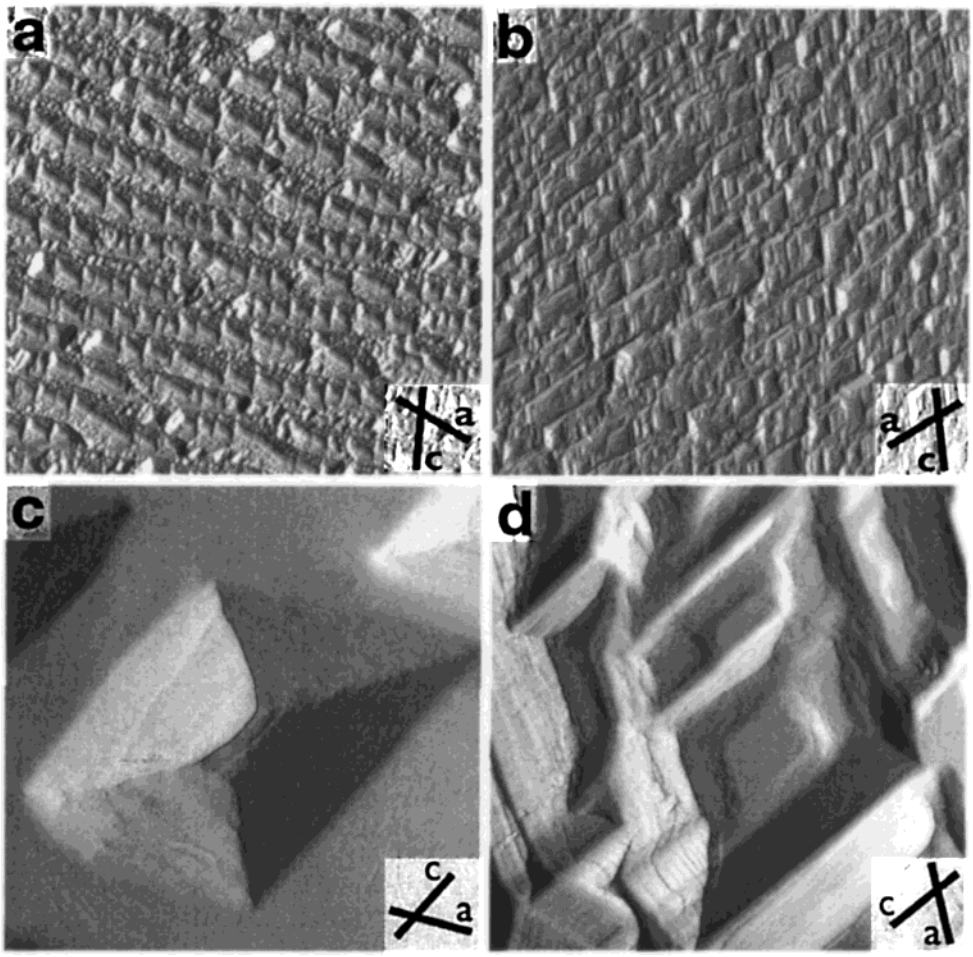

Figure 5. AFM images of the (010) face of four different acetaminophen single crystals dissolved in water: a 55 × 55 μm^2 scan for 60 s at 30 °C (a); a 60 × 60 μm^2 scan for 15 s at 30 °C (b); a 2 × 2 μm^2 scan for 30 s at 40 °C (c); a 5 × 5 μm^2 scan for 30 s at 30 °C (d). The *a* and *c* axes are marked on each image.

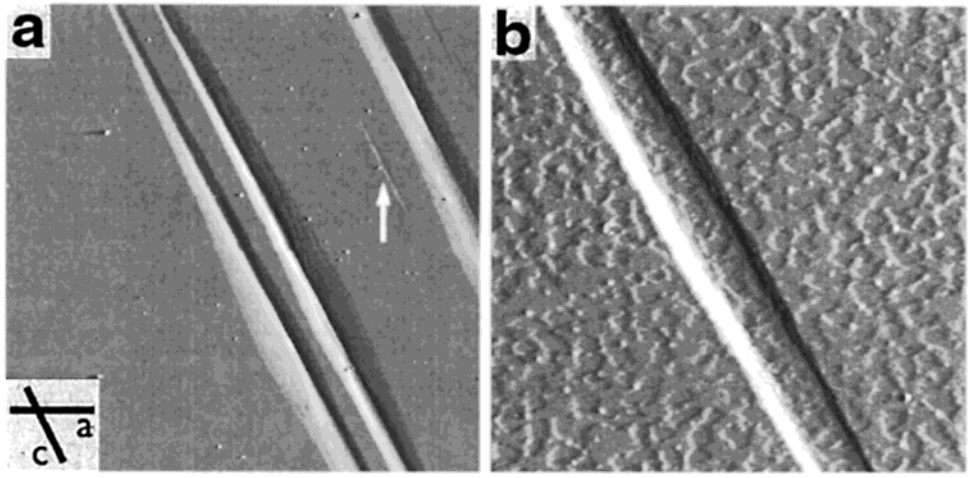

Figure 6. AFM images of the (010) face of an acetaminophen single crystal dissolved in dichloroethane for 60 s at 20 °C: a 60 × 60 μm^2 scan (a); a zoomed-in 5 × 5 μm^2 scan (b). A white arrow points where (b) was taken from (a). The *a* and *c* axes are marked on (a).

nophen crystal after partial dissolution in pyridine/CCl_4 (1:5 v/v). The etching pattern is regular, and the shape resembles a hexagon. Of the six sides of the hexagon, two are parallel to the *a* axis and two are parallel to the *c* axis. A lower magnification image shows a big pit containing a few smaller ones (Figure 7a). The higher magnification image in Figure 7b shows layers of the crystal around the core of etch pits. Each layer is approximately as high as the long dimension of the unit cell. Image analysis indicates that each layer in the middle of Figure 7b is about 10 Å. It suggests that the crystal is dissolved a layer of unit cells or even a layer of molecules at a time. It is not clear at this moment, however, whether a layer of unit cells is dissolved at once or the bottom layer of molecules within the same layer of unit cells becomes unstable after the top layer is dissolved.

Four AFM images of cleaved (010) faces of two acetaminophen crystals after dissolution in acetone/CCl_4 (1:1 v/v) show a square shaped etching pattern (Figure 8). Two sides of the

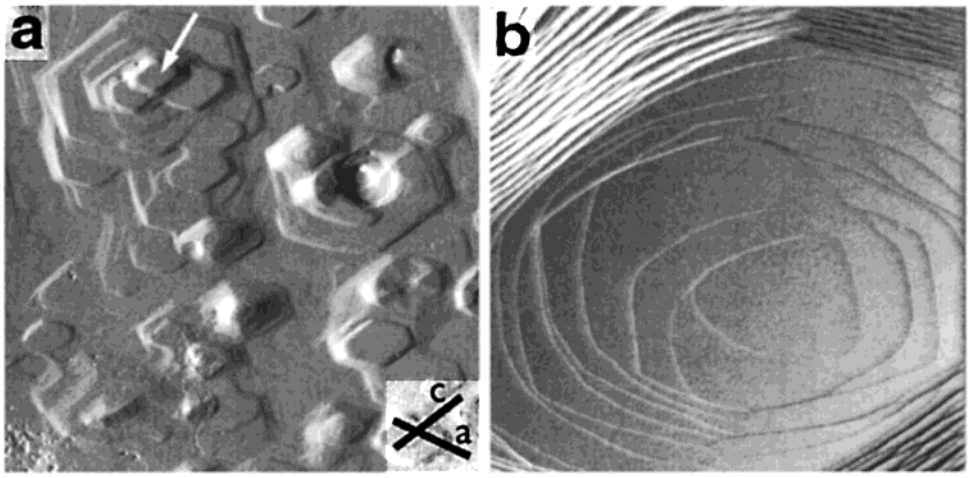

Figure 7. AFM images of the (010) face of an acetaminophen single crystal dissolved in pyridine/CCl_4 (1:5 v/v) for 30 s at 20 °C: a 60 × 60 μm^2 scan (a); a zoomed-in 3.5 × 3.5 μm^2 scan (b). A white arrow points where (b) was taken from (a). The *a* and *c* axes are marked on (a).

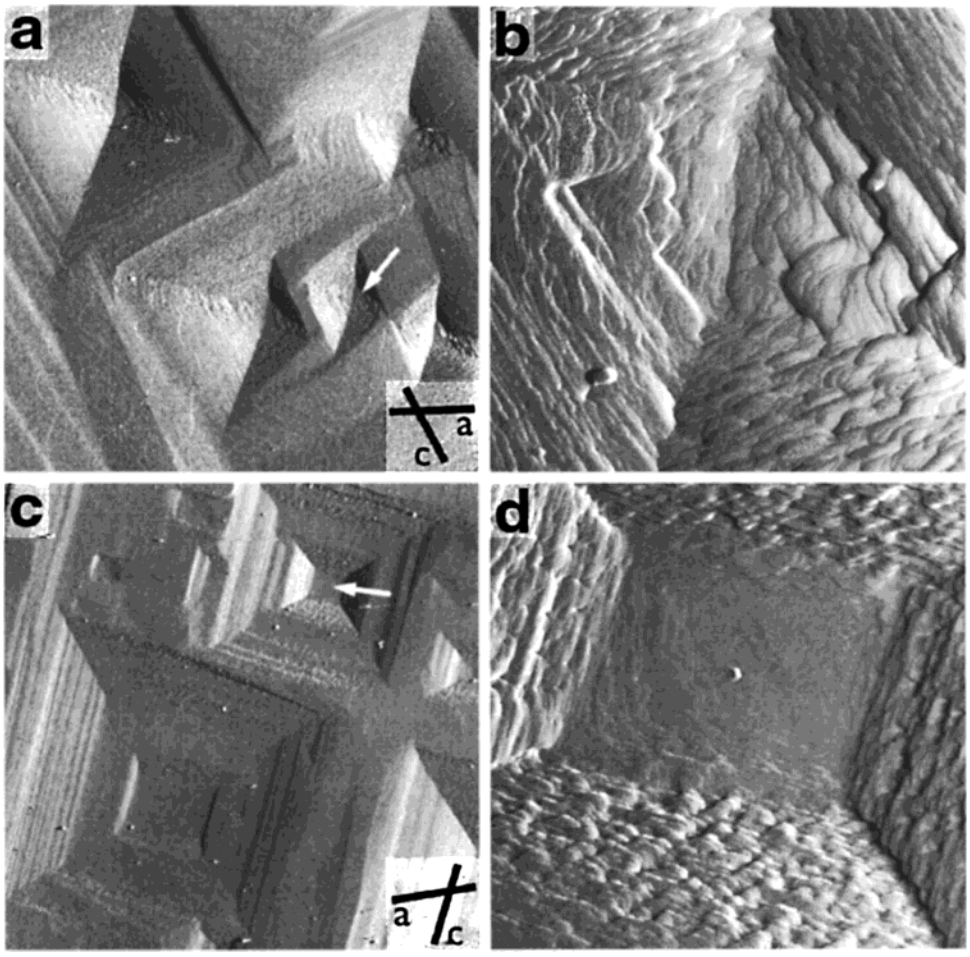

Figure 8. AFM images of the (010) face of two acetaminophen single crystals dissolved in acetone/CCl_4 (1:1 v/v) for 5 (a and b) and 15 (c and d) seconds at 20 °C, respectively. (b) A 5 × 5 μm^2 scan, was zoomed in from (a), a 50 × 50 μm^2 scan. (d) A 7.5 × 7.5 μm^2 scan, was zoomed in from (c), a 60 × 60 μm^2 scan. The white arrows show where the zooming is. The *a* and *c* axes are marked on (a) and (c), respectively.

etch pits are parallel to the *c* axis of the crystal. However, it seems that, again, there is no texture feature related to the *a* axis. Some etch pits look like an inverted pyramid (Figure 8a), but some have a relatively flat bottom (Figure 8c). Cleaved (010) faces of the two acetaminophen crystals after dissolution in ethyl acetate/CCl_4 (1:1 v/v) show a rectangular shaped etching pattern (Figure 9). Two sides of the etch pits are parallel to the *c* axis of the crystal. There appear to be no features related to the *a* axis. The ledges parallel to the *c* axis are longer than those perpendicular to the *c* axis. The centers of the etch pits are relatively flat. Figure 10 shows the cleaved (010) faces of an acetaminophen crystal after partial dissolution in acetic anhydride/CCl_4 (1:1 v/v). The etching pattern is regular, and the shape generally resembles a parallelogram. Two sides of etch pits are parallel to the *a* axis and other two parallel to the *c* axis of the crystal.

The AFM observations show that etching patterns formed by dissolution on the (010) face of acetaminophen crystals are

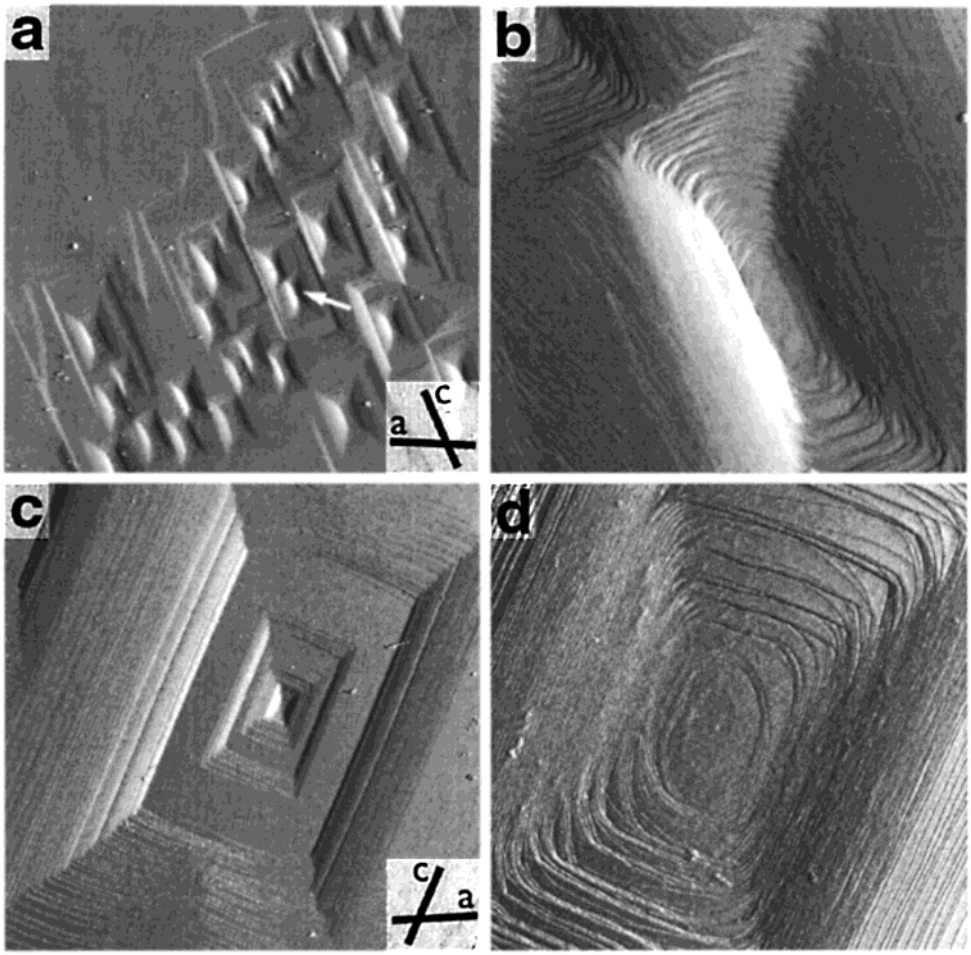

Figure 9. AFM images of the (010) face of two acetaminophen single crystals dissolved in ethyl acetate/CCl_4 (1:1 v/v) for 5 (a and b) and 15 (c and d) seconds at 20 °C, respectively. (b) A 5 × 5 μm^2 scan, was zoomed in from (a), a 70 × 70 μm^2 scan. (d) A 3.5 × 3.5 μm^2 scan, was zoomed in from (c), a 60 × 60 μm^2 scan. The white arrows show where the zooming is. The *a* and *c* axes are marked on (a) and (c), respectively.

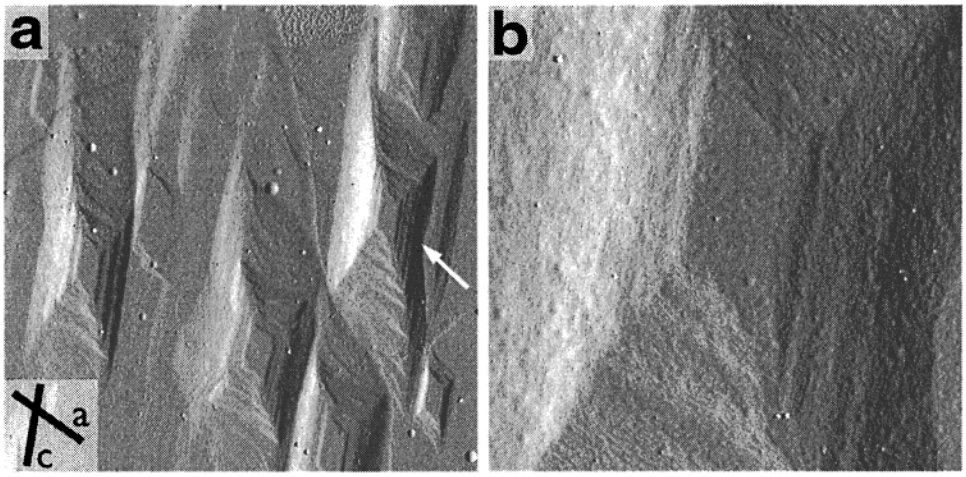

Figure 10. AFM images of the (010) face of an acetaminophen single crystal dissolved in acetic anhydride/CCl_4 (1:1 v/v) for 20 s at 20 °C: a 50 × 50 μm^2 scan (a); a zoomed-in 10 × 10 μm^2 scan (b). A white arrow points where (b) was taken from (a). The *a* and *c* axes are marked on (a).

regular. Different solvents caused different shapes of etch pits, such as parallelogram (in water and acetic anhydride), slit (in dichloroethane), hexagonal (in pyridine), square (in acetone), and rectangular (in ethyl acetate). Furthermore, all etching patterns are related to the crystal structure. Dichloroethane, acetone, and ethyl acetate resulted in shapes of etch pits parallel to the *c* axis only. Water, pyridine, and acetic anhydride, on the other hand, resulted in shapes of etch pits parallel to the *a* and *c* axes. The dissolution mechanism appears to be controlled by both the underlying crystal structure and the solvent used. This will be discussed later.

Simulated Etching Patterns. Simulated etched surfaces under different surface diffusion modes are shown in Figure 11. The top and bottom edges of all the simulated models in this report are parallel to the *a* axis, and two side edges are parallel to the *c* axis of the acetaminophen model. The solid−liquid interaction was set to −40 kcal/mol. For the three models with surface diffusion considered, the diffusion area (which is

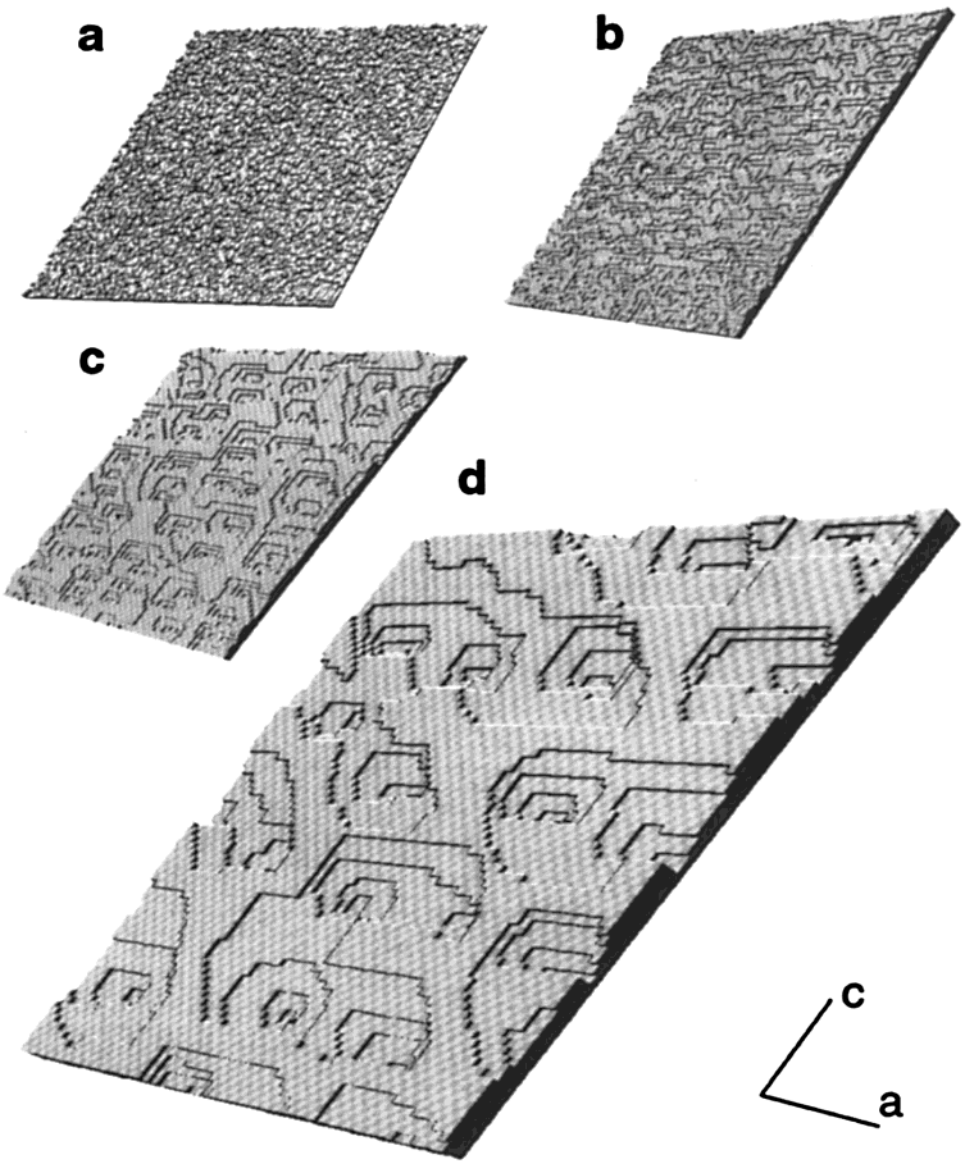

Figure 11. Surface models simulated to study the effect of surface diffusion mode: no surface diffusion (a); weak surface diffusion (b); medium surface diffusion (c); strong surface diffusion (d) (enlarged to show the pits). Directions of the *a* and *c* axes of each model are roughly marked.

the area that a newly dissolved crystal molecule to diffuse) was set to 20 × 20. The diffusion number, which is the number of molecules allowed to diffuse, was set to 100. Another diffusion parameter, diffusion length, which is the area where a diffusing molecule is confined to move in the strong and medium diffusion modes, was set to 20 × 20. In the weak diffusion mode, diffusion length, which is the number to repeat the locally equilibrating move, was set to 10. These simulated surface models reveal that implementing a different diffusion mode or mechanism can affect the etching pattern. If no surface diffusion but only detachment is considered, there is no regular etching pattern at all (Figure 11a). When surface molecules are allowed to diffuse, etching patterns appear (Figure 11b−d). In addition, when the diffusion is treated as more than a local thermal event (i.e., from the weak to the medium to the strong diffusion mode), the etching pattern becomes larger. The shape of the etching pattern is regular and all etch pits are similar, as shown in parts c and d of Figure 11. The general shape is hexagonal with two edges parallel to the *a* axis (overlapping with one hydrogen bonding direction) and two parallel to the *c* axis. The latter two edges are zigzagged along another hydrogen-bonding direction. Another feature of etch pits is that the shape or geometry is not symmetric. Those pits bisected by the right side edge, as shown in Figure 11d, demonstrate this feature. The asymmetry is commonly observed for all the simulated pits in this study. Nevertheless, it should be pointed out that all the simulated models shown in the paper were computed with the interlayer jumping option disabled. In fact, when this "jump down" option was enabled, the etch pits were only one-layer high and no deep ones were formed. The reason was that after a molecule was detached from a lower layer, there was a surface molecule that diffused and filled the hole quickly. The resulting etch pits were, therefore, only one layer high, and the surface model was dissolved by a layer-by-layer mechanism. Since the actual etching patterns did not show the layer-by-layer dissolution, "jumping down" does not appear to be dominant in real dissolution processes. It is possible as well that, after jumping down, the desorbed surface molecule goes to the solvent directly.

The effect of diffusion number on the etching pattern is shown in Figure 12. The solid−liquid interaction was set to −40 kcal/mol, and the strong diffusion mode was used. Random walking was conducted until the last layer of each model started to dissolve. The diffusion area and diffusion length were both set to 20 × 20. The diffusion numbers were set to 25 (Figure 12a),

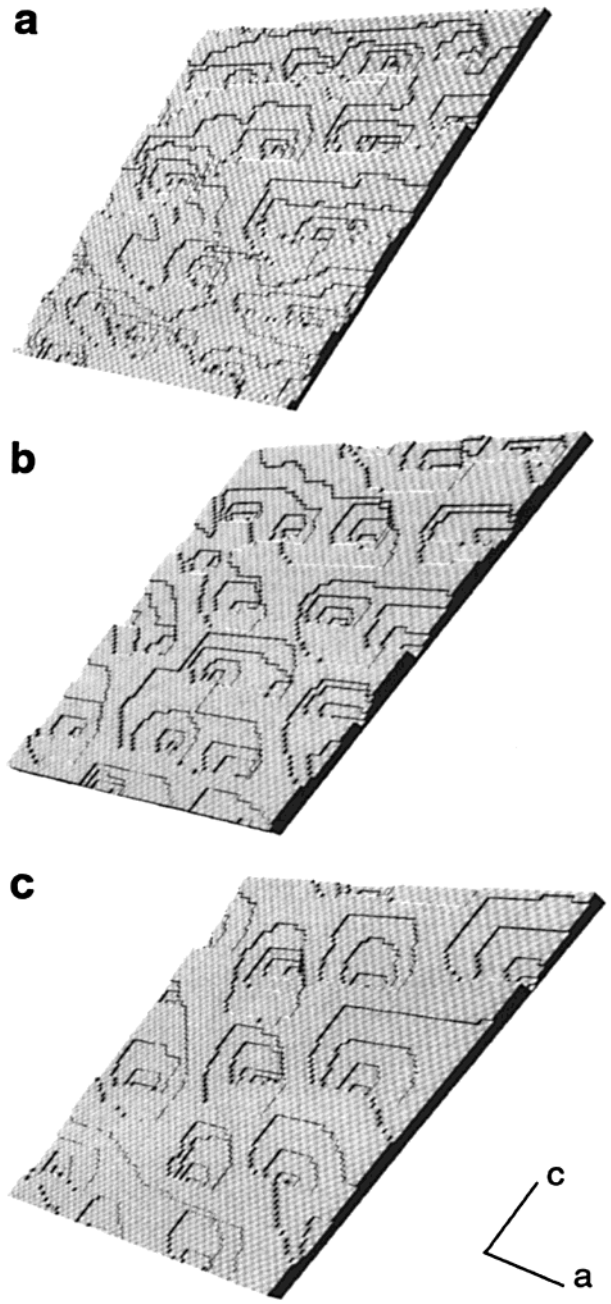

Figure 12. Surface models simulated to study the effect of diffusion number: 25 (a); 100 (b); 400 (c). Directions of the *a* and *c* axes of each model are roughly marked.

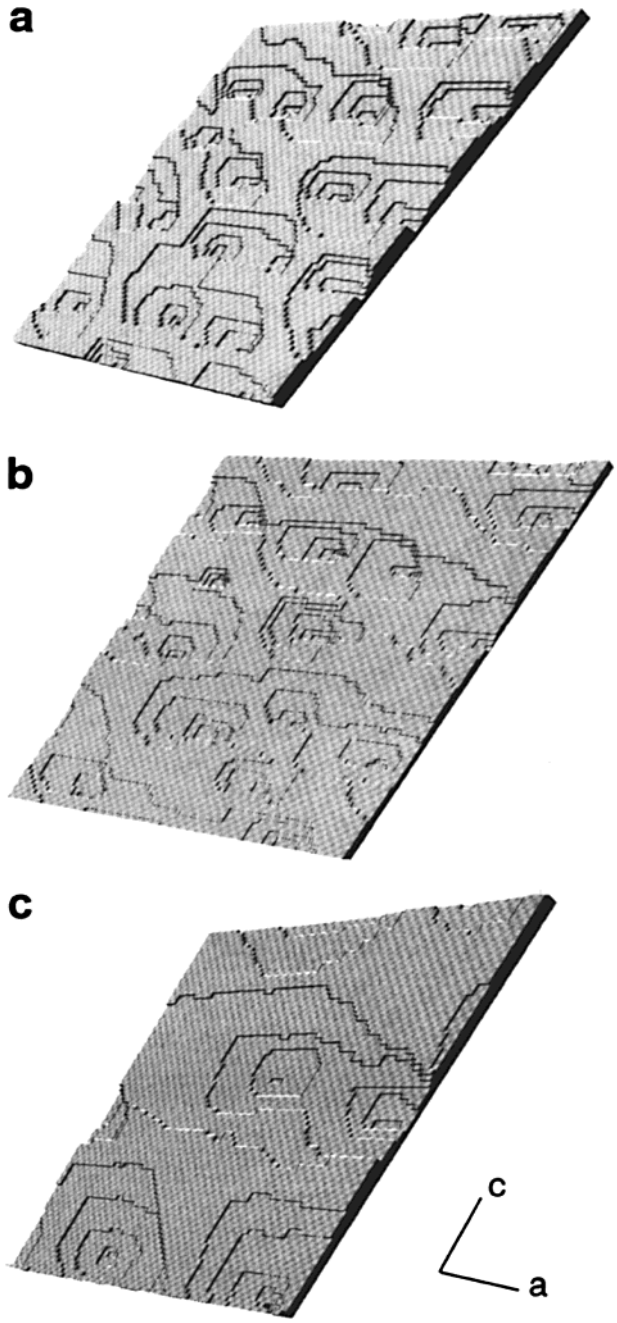

Figure 13. Surface models simulated to study the effect of diffusion area and diffusion length: 20 × 20 and 20 × 20 (a); 50 × 50 and 20 × 20 (b); 20 × 20 and 50 × 50 (c). Directions of the *a* and *c* axes of each model are roughly marked.

100 (Figure 12b), and 400 (Figure 12c). The diffusion number clearly affects the formation of etched patterns. The general trend is that the etch pits become larger and fewer per unit surface area as the diffusion number is increased. The more molecules diffused, the larger were the etch pits. Because the diffusion area was set to 20 × 20, the maximum number of surface molecules considered for surface diffusion around a newly dissolved surface site was 400. Therefore, in the model shown in Figure 12c, almost all surface molecules within the diffusion area were considered for surface diffusion.

The effects of the diffusion area and diffusion length on the etching pattern are illustrated in Figure 13. The solid−liquid interaction was set to −40 kcal/mol and the strong diffusion mode was used for the three models. Random walking was conducted until the last layer of each model started to dissolve. The diffusion number was set to 100 for all three models. Both diffusion area and length were set to 20 × 20 for the model in Figure 11a. The diffusion area was set to 50 × 50, and diffusion length was kept at 20 × 20 for the model in Figure 13b. For the model in Figure 13c, however, the diffusion area was kept at 20 × 20 while the diffusion length was changed to 50 × 50. Comparison of the three surface models shows that increasing the diffusion length can enlarge the etch pits and, therefore, reduce the number of etch pits per unit surface area. Nevertheless, increasing the diffusion area seems ineffective in reshaping the etch pits if the diffusion number is kept fixed. Obviously, if molecules still diffuse the same distance, changing diffusion area to select the same number of molecules should not affect the etching patterns much. On the other hand, if diffusion length is increased, the etch pits are enlarged even with an equal number of molecules participating in surface diffusion.

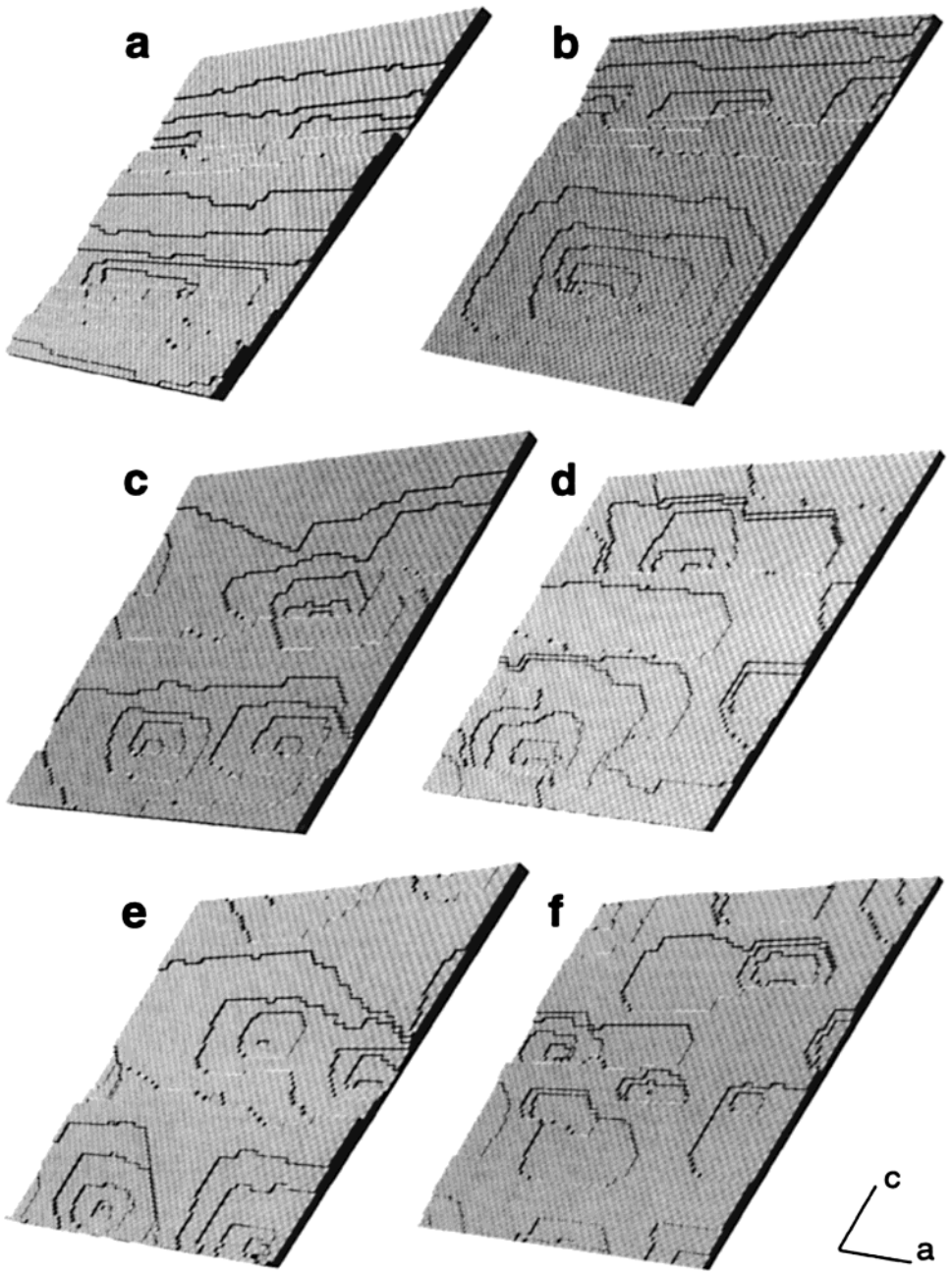

Figure 14. Surface models simulated to study the effect of solid−liquid interaction: −30.0 kcal/mol (a); −32.5 kcal/mol (b); −35.0 kcal/mol (c); −37.5 kcal/mol (d); −40.0 kcal/mol (e); −42.5 kcal/mol (f). Directions of the *a* and *c* axes of each model are roughly marked.

The effect of solid−liquid interaction parameter on formation of etching patterns is shown in Figure 14. The strong diffusion mode was used, and the diffusion parameters were 20 × 20 for the diffusion area, 100 for the diffusion number, and 50 × 50 for the diffusion length. Random walking was conducted until the last layer of each model started to dissolve. The solid−liquid interaction was set to −30.0 (Figure 14a), −32.5 (Figure 14b), −35.0 (Figure 14c), −37.5 (Figure 14d), −40.0 (Figure 14e), and −42.5 kcal/mol (Figure 14f). Apparently, the solid−liquid interaction plays a very important role in controlling the formation of etch pits and the shape of etching patterns. When the absolute value of solid−liquid interaction is increased, the shape of etch pits becomes shorter along the *a* axis but becomes longer along the *c* axis. The elongation along the *c* axis is extremely limited when the absolute value of solid−liquid interaction is the smallest, 30 kcal/mol, as shown in Figure 14a. The domination of elongation along the *a* axis is still apparent when the absolute value of solid−liquid interaction is increased to 40.0 kcal/mol. Elongation along another hydrogen-bonding direction appears as the solid−liquid interaction increased. It is also interesting to notice that the number of etch pits is increased as the solid−liquid interaction increased. This is due to the increased success ratio of detachment at high interaction. When the absolute value of solid−liquid interaction was increased to 42.5 kcal/mol, any surface molecule chosen was able to be dissolved.

Discussion

The etching patterns on the (010) face of acetaminophen single crystals created by partial dissolution have regular shapes. The shape of etch pits varies depending upon the solvent used. All etching patterns observed appear to be related to the underlying crystal structure. Computer simulation suggests that the surface diffusion is the essential event in determining the shape of the etch pits. Equally important is that the interaction

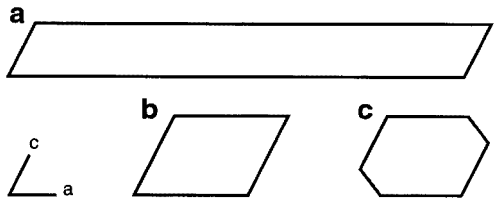

Figure 15. Three simulated etching patterns of the (010) face of acetaminophen. Directions of the *a* and *c* axes are shown.

network among molecules in the crystal lattice in part controls the shape of etch pits formed on the (010) face of acetaminophen single crystals. The direction of a ledge or a side of a pit is aligned with one axis of the interaction network such as the *a* axis or *c* axis. When a molecule (e.g., labeled #1 in Figure 1) is diffusing on the crystal surface, it can migrate and occupy two possible energy-favored empty sites, marked by α and β in Figure 1. If a 2D network of molecular interactions exists within each layer and the attractive force along the *x* axis is stronger than the attractive force along the *y* axis, the #1 molecule will diffuse into and stay at site β. Binding with its neighbor molecules is much tighter than binding in site α. Furthermore, in the event of detachment, molecules in ledges along the *y* axis are more easily removed than molecules in ledges along the *x* axis. This suggests that if a poor solvent is used to dissolve the crystal, ledges along the *x* axis will be much longer than those along the *y* axis. As the solvent quality is improved, ledges along the weak force direction appear and become longer. The simulation results shown in Figure 14 demonstrate this trend.

On the basis of the simulation, it is expected that etching patterns on the (010) face of acetaminophen should be close to one of those shown in Figure 15. Formation of different shapes depends on the strength of the interaction between the crystal and the solvent. It can be a parallelogram with longer sides parallel to the *a* axis, as formed by a poor solvent, or, it can be a parallelogram with sides of similar lengths, as formed by an intermediate solvent. It can also be a hexagon, as formed by a good solvent, with two sides parallel to the *a* axis, two parallel to the *c* axis, and the remaining two parallel to the hydrogen-bonding direction that is not the one along the *a* axis. Etching experiments show that etching patterns of the (010) faces dissolved by water and acetic anhydride may correspond to Figure 15b. The etching pattern by pyridine matches with the one in Figure 15c. This may be confirmed by the fact that the solubility values of acetaminophen in water and acetic anhydride are very close and the solubility in pyridine is the highest. Etching patterns of the (010) faces of acetaminophen single crystals dissolved in dichloroethane, acetone, and ethyl acetate, however, are much different from the simulation. Even more surprisingly, there is no surface feature that could be related to the *a* axis of the crystal structure. The etching pattern by dichloroethane, which is a poor solvent for acetaminophen (Table 2), should be close to the one shown in Figure 15a. Instead, the experimentally observed pattern shows a long, narrow slit along the *c* axis. Moreover, as indicated from the computation of intermolecular interactions shown in the force matrix, interactions along the *a* axis are actually the strongest. The simulation suggests that, because of surface diffusion, the shape of an etch pit is confined or bounded by the interaction network and mainly by interactions along the *a* axis. For the formation of etching patterns by dichloroethane, acetone, and ethyl acetate, there might be other factors that interfere with the expected elongation based on the intermolecular interactions. It is possible that the solvent molecules adsorb to the crystal

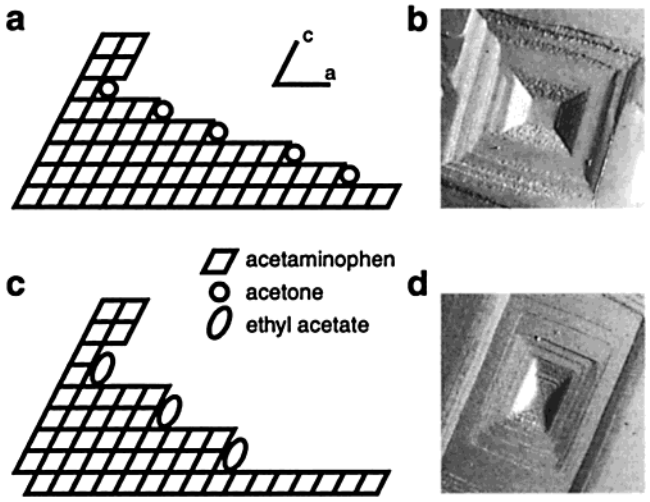

Figure 16. Schematic illustration of blocking of ledges along the *a* axis by acetone (a) and ethyl acetate (c) on the (010) face of acetaminophen. Corresponding AFM images are also shown: a 30 × 30 μm^2 scan after dissolved in acetone (b); a 15 × 15 μm^2 scan after dissolved in ethyl acetate (d).

surface and block the continuation of ledges formed on the (010) face. Dichloroethane does not have the ability to form any hydrogen bonding with other molecules. When a dichloroethane molecule diffuses to an empty site in a ledge along the *a* axis, it may block the elongation of the ledge and make it unstable due to the discontinuation of hydrogen bonding. Nevertheless, the dichloroethane molecule can still bind with acetaminophen molecules through van der Waals force. When it diffuses to a site in a ledge along the *c* axis, the elongation may continue because van der Waals is the dominant force along this direction. This may be the reason that etch pits by dichloroethane resemble a narrow band or a slit along the *c* axis.

For acetone and ethyl acetate, if they adsorb to the surface when forming an etch pit, their influence may be different from that of dichloroethane. Two solvents can bind to acetaminophen molecules through van der Waals as well as hydrogen bonding. Acetone and ethyl acetate, however, cannot propagate the hydrogen-bonding network since they can only provide lone pair electrons. Thus, they can act as terminators of the hydrogen bonding network. As shown in Figure 16a, when an acetone molecule diffuses into an empty site of a ledge along the *a* axis, it may bind to the left acetaminophen molecule and terminate the elongation to the right. Like dichloroethane, acetone participates in the propagation of van der Waals along the *c* axis. As a result, ledges along the *c* axis are straight while ledges along the *a* axis are zigzagged. The direction of the zigzagged outline maybe then was away from the *a* axis. On a large scale, this may form the etching pattern shown in Figure 8 (also shown in Figure 16b). The same mechanism may apply to the formation of etch pits by ethyl acetate. But, it may terminate hydrogen bonding along one edge and block another neighboring one, as shown in Figure 16c. This is because it has a larger volume than acetone, as shown in Table 2. The elongation along the *a* axis is then kinetically slowed compared to that observed with acetone. As a result, ledges along the *c* axis are straight and longer, while ledges along the *a* axis make up a shorter zigzagged outline shown in Figure 9 (also shown in Figure 16d). The direction of the observed "zigzagged" ledges is between the two hydrogen bonding routes. As seen from Figure 16, it is possible that either acetone or ethyl acetate could terminate acetaminophen ledges on the left as well. It may be that the ledges terminated on the left are less stable than those terminated

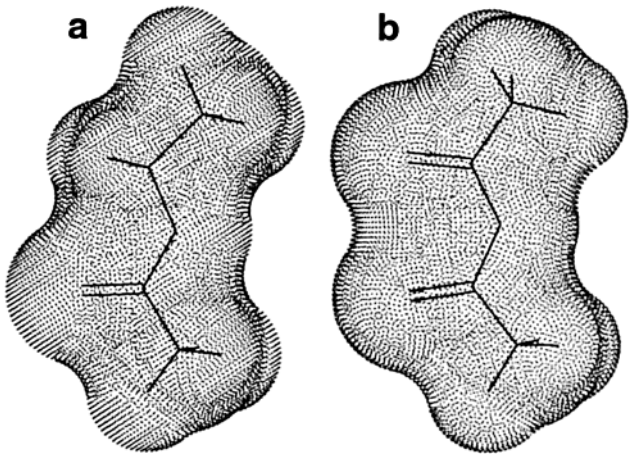

Figure 17. Connolly surfaces of ethyl acetate (a) and acetic anhydride (b).

on the right (as observed), since otherwise the second hydrogen bonding direction would be exposed.

As indicated in Table 2, molecules of all solvents used in the dissolution experiments are smaller than the acetaminophen molecule. However, it appears that not only does a solvent molecule have to be small enough to fit in the vacancy on the crystal surface but also it should have unique structural properties to fit in the supramolecular motif of the crystal structure to alter the shape of etch pits from the model's "ideal". Ethyl acetate and acetic anhydride show similar solubility values for acetaminophen (Table 2). In addition, they have roughly the same molecular volume (Table 2). Their structural difference (i.e., a methylene group vs a carbonyl group as shown in Figure 17), however, causes the dramatic dissimilarity between the etching patterns by the solvents. Because of the second carbonyl group, it might be difficult for acetic anhydride molecules to adsorb to the crystal surface and modify the molecular interaction network of acetaminophen single crystals. Even if a solvent molecule can fit in the supramolecular motif, its role in affecting surface morphology may be decided by how frequent the adsorption event is with respect to other events. Pyridine molecules might be able to adsorb to the crystal surface and take part in the supramolecular motif. However, the adsorption of pyridine molecules may be trivial since acetaminophen can be dissolved in pyridine so fast and in such a large amount (Table 2). For dichloroethane molecules, the adsorption might be the dominant event.

Dissolution is a process where both molecules in the crystal and solvent molecules affect the formation of surface morphology and surface texture. The crystal structure and underlying molecular interactions control the dissolution process. Surface diffusion is the key event in forming etching patterns and molecules are confined to diffuse by the supramolecular interaction network. The simulation indicates that, if surface molecules diffuse longer, more frequently, and more actively, the formed etch pits will be larger and more regular. Although a few diffusion mechanisms have been proposed and implemented in the simulations, the diffusion behavior is certainly more complicated in the real systems. As an intrinsic property, surface diffusion can be affected by the crystal structure, the solvent, and experimental conditions. Among various environmental parameters, temperature can influence the diffusion coefficient significantly and may, in turn, affect the etching patterns. Studying the effect of temperature on surface diffusion can be very important, as it has been known that increasing temperature can cause the surface roughness transition for crystal growth while the quantitative understanding of it is very limited.[9] It is possible that the order−disorder transition is caused by changes of surface diffusion behavior of surface molecules. Undoubtedly, investigating etching patterns would provide helpful information to answer such question as surface roughening.

The role of solvent molecules is determined by their abilities to interact with surface molecules. If solvent molecules could be adsorbed and bounded onto the crystal face, their interactions with molecules may transform the original interaction network (e.g., hydrogen bonding network) into a new motif, which, in turn, mutates the shape of etch pits. It is indicated that the number of kinks along steps or dissolution fronts is decided by temperature, crystallographic orientation, and binding energy parameters.[7] Thus, the solid−solvent interaction can affect the kink density along different steps and, thus, control the regressive velocities of relevant steps. Adsorption of solvent or impurity molecules on kink sites of some particular steps can influence the stability and vary regressive velocities of the steps so that the shape of etch pits is changed. Understandings of how the supramolecular structure controls physicochemical properties of the crystal can be applied to utilizing additives to control the shape of etch pits[32,33] and the morphology of crystals such as acetaminophen[34] and L-alanine.[35] In fact, designing molecular crystals with various properties by controlling the hydrogen bonding network has become very successful.[36−38]

Summary

This study suggests that the experimentally observed etching patterns may result from surface diffusion of crystal molecules desorbed during the dissolution process. The diffusion is guided or confined by underlying crystal structures, especially the supramolecular interaction network. In addition, the solvent−crystal interaction affects the formation of etch pits and plays an important role in determining the detachment and surface diffusion of surface molecules. Our data suggest that solvent molecules may be adsorbed on the crystal surface and influence the surface morphology. If a solvent molecule can "recognize" a surface site and join the supramolecular motif of the crystal surface, it may alter the original interaction network and in turn, change the etching pattern. Therefore, the dissolution mechanism at the crystal surface is not only affected by the solvent−solid interaction but also controlled by the crystal structure and the mutual recognition between solvent molecules and molecules in the crystal.

Acknowledgment. This study was supported by the NSF/Industry/University Cooperative Research Center for Pharmaceutical Processing at Purdue University.

References and Notes

(1) Sangwal, K.; Rodriguez-Clemente, R. *Surface Morphology of Crystalline Solids*; Trans Tech Publications: Zürich, 1989.

(2) *Advances in the Understanding of Crystal Growth Mechanisms*; Nishinaga, T., Nishioka, K., Harada, J., Sasaki, A., Takei, H., Eds.; Elsevier: Amsterdam, 1997.

(3) Wurster, D. E.; Taylor, P. W. *J. Pharm. Sci.* **1965**, *54*, 169−175.

(4) Noyes, A.; Whitney, W. R. *J. Am. Chem. Soc.* **1897**, *19*, 930−934.

(5) Wurster, D. E.; Kildsig, D. O. *J. Pharm. Sci.* **1965**, *54*, 1491−1494.

(6) Higuchi, W. I. *J. Pharm. Sci.* **1967**, *56*, 315−324.

(7) Burton, W. K.; Cabrera, N.; Frank, F. C. *Philos. Trans. R. Soc. London, Ser. A* **1951**, *243*, 299−358.

(8) Frank, F. C. On the Kinematic Theory of Crystal Growth and Dissolution Processes. In *Growth and Perfection of Crystals*; Doremus, R.

H., Roberts, B. W., Turnbull, D., Eds.; John Wiley & Sons: New York, 1958; pp 411−417.
(9) Roberts, K. J.; Docherty, R.; Bennema, P.; Jetten, L. A. M. J. *J. Phys. D: Appl. Phys.* **1993**, *26*, B7−B21.
(10) Somorjai, G. A. *Introduction to Surface Chemistry and Catalysis*; John Wiley & Sons: New York, 1994.
(11) Somorjai, G. A. *J. Mol. Catal. A: Chem.* **1996**, *107*, 39−53.
(12) Somorjai, G. A. *MRS Bull.* **1998**, *23*, 11−29.
(13) Kardar, M.; Parisi, G.; Zhang, Y. C. *Phys. Rev. Lett.* **1986**, *56*, 889−892.
(14) Barabási, A.-L.; Stanley, H. E. *Fractal Concepts in Surface Growth*; Cambridge University Press: Cambridge, UK, 1995; p 150.
(15) Barabási, A.-L.; Stanley, H. E. *Fractal Concepts in Surface Growth*; Cambridge University Press: Cambridge, UK, 1995.
(16) Kohli, C. S.; Ives, M. B. *J. Cryst. Growth* **1972**, *16*, 123−130.
(17) Gilmer, G. H.; Bennema, P. *J. Appl. Phys.* **1972**, *43*, 1347−1360.
(18) Creus, A. H.; Carro, P.; Salvarezza, R. C.; Arvia, A. J. *Langmuir* **1997**, *13*, 833−841.
(19) Meyer, E. *Prog. Surf. Sci.* **1992**, *41*, 3−49.
(20) Radmacher, M.; Tillmann, R. W.; Fritz, M.; Gaub, H. E. *Science* **1992**, *257*, 1900−1905.
(21) *Atomic Resolution Microscopy of Surfaces and Interfaces*; Smith, D. J., Ed.; Materials Research Society: Pittsburgh, 1997; Vol. 466.
(22) Carter, P. W.; Hillier, A. C.; Ward, M. D. *J. Am. Chem. Soc.* **1994**, *116*, 944−953.
(23) Gratz, A. J.; Manne, S.; Hansma, P. K. *Science* **1991**, *251*, 1343−1346.
(24) Haisa, M.; Kashino, S.; Kawai, R.; Maeda, H. *Acta Crystallogr.* **1976**, *B32*, 1283−1285.
(25) Russell, V. A.; Ward, M. D. *Chem. Mater.* **1996**, *8*, 1654−1666.
(26) Ward, M. D. *Curr. Opin. Colloid Interface Sci.* **1997**, *2*, 51−64.
(27) Fairbrother, J. E. Acetaminophen. In *Analytical Profiles of Drug Substances*; Florey, K., Ed.; Academic Press: New York, 1974; Vol. 3, pp 2−109.
(28) Duncan-Hewitt, W. C.; Mount, D. L.; Yu, A. *Pharm. Res.* **1994**, *11*, 616−623.
(29) Bennema, P. *J. Cryst. Growth* **1996**, *166*, 17−28.
(30) Metropolis, N.; Rosenbluth, A. W.; Rosenbluth, M. N.; Teller, A. H. *J. Chem. Phys.* **1953**, *21*, 1087−1092.
(31) Cormen, T. H.; Leiserson, C. E.; Rivest, R. L. *Introduction to Algorithms*; MIT Press: Cambridge, 1991.
(32) Weissbuch, I.; Popovitz-Biro, R.; Lahav, M.; Leiserowitz, L. *Acta Crystallogr.* **1995**, *B51*, 115−148.
(33) Shimon, L. J. W.; Lahav, M.; Leiserowitz, L. *J. Am. Chem. Soc.* **1985**, *107*, 3375−3377.
(34) Hendriksen, B. A.; Grant, D. J. W.; Meenan, P.; Green, D. A. *J. Cryst. Growth* **1998**, *183*, 629−640.
(35) Lechuga-Ballesteros, D.; Rodríguez-Hornedo, N. *Int. J. Pharm.* **1995**, *115*, 151−160.
(36) Etter, M. C.; Reutzel, S. M. *J. Am. Chem. Soc.* **1991**, *113*, 2586−2598.
(37) Etter, M. C. *J. Phys. Chem.* **1991**, *95*, 4601−4610.
(38) Russell, V. A.; Etter, M. C.; Ward, M. D. *Chem. Mater.* **1994**, *6*, 1206−1217.